JOURNAL OF MATERIALS RESEARCH AND TECHNOLOGY 2022;19:2247–2256

Available online at www.sciencedirect.com

jmr&t
Journal of Materials Research and Technology

journal homepage: www.elsevier.com/locate/jmrt

Original Article

Optimization of the chemical composition of a commercial AA6060 alloy to maximize extrudability and mechanical properties

C. Menapace [a,*], F. Bernard [b], M. Lusa [b], G. Straffelini [a]

[a] University of Trento, Department of Industrial Engineering, Via Sommarive 9, 38123 Trento, Italy
[b] Pandolfo Alluminio SpA, Via Camp Lonc 23, 32032 Feltre (BL), Italy

ARTICLE INFO

Article history:
Received 30 March 2022
Accepted 2 June 2022
Available online 9 June 2022

Keywords:
6060 Al alloy
Chemical composition
Ageing treatment
Extrudability
Pick-up
die lines

ABSTRACT

A new AA6060 alloy composition was proposed modifying a standard composition in which the Mg and Si contents were reduced to the minimum level allowed, with the aim to increase the alloy extrudability and reduce the extrusion time. With the novel composition extruded Al profiles were manufactured, from which tensile test samples were cut. Applying a proper ageing cycle, mechanical properties higher than the minimum values required for this alloy were achieved, also in the case of the minimum Mg + Si content.

A significant improvement in extrudability was observed reducing the amounts of Mg and Si. The low content of these alloying elements led to a consistent increase in the extrusion velocity exploitable without the occurrence of any surface defect. A temperature model has been formulated to describe the appearance of defects on the surface of the extruded profiles like die lines and pick-ups.

1. Introduction

Products that use aluminum alloys are widely fabricated by hot extrusion, suitable to obtain accurate profiles and complex shapes. Hot extrusion is a plastic deformation process in which a billet is pressed through a die opening to create the desired shape [1]. When aiming to enhance its productivity, an aluminum extrusion plant goes for high extrudability alloys – i.e. alloys extruded with the highest extrusion speed suitable before the first surface defect appearing – while satisfying the minimum mechanical properties requirements. The lower is the extrusion time, the higher will be the plant's productivity but the alloys extrudability must be preserved. As reported in Fig. 1 [2] the simplified extrusion limit diagram identifies a working range in which the metallurgical limitations at high temperatures are related to the following phenomena: (a) tearing, (b) die pick-up and die lines, (c) surface recrystallization. Tearing – also known as hot shortness [3] or speed cracking [4] – is a surface defect related to temperature: it occurs when the exit temperature of the extruded profile overcomes a critical value, that is the temperature at which the hot ductility of the aluminum alloy falls below the level required to withstand the strains imposed by the extrusion process [4]. This critical temperature is equivalent to the solidus temperature in a low solute alloy like the 6060 [4,5], whereas in a high solute alloy, like for example the 6082, due

* Corresponding author.
E-mail address: cinzia.menapace@unitn.it (C. Menapace).
https://doi.org/10.1016/j.jmrt.2022.06.014

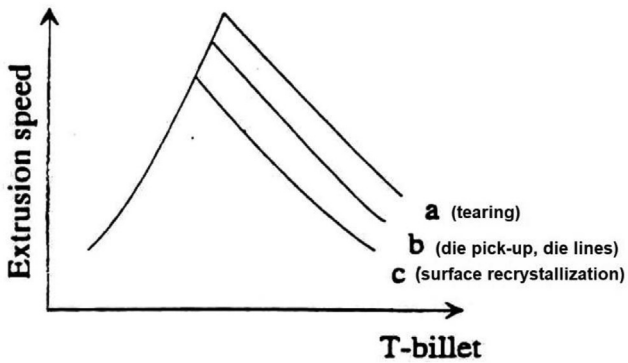

Fig. 1 – Metallurgical limitations for extrusion limit diagram [2].

to the presence of low melting point phases, it corresponds to the eutectic temperature – being the tearing phenomenon associated to the incipient melting of these phases [6,7]. Tearing can be visible in the inner hollow sections as well as on the outer edges of extruded profiles – i.e. the regions in which, generally, higher temperatures are reached – and it can be linked to a roughening of the extrusion surface. Tearing phenomena result in the appearance of cracks [8–10].

Die pick-ups and die lines are surface defects, which have the appearance of scratch marks. Die lines are continuous deep grooves parallel to the extrusion direction. These defects are ascribed to the interaction of the extrudate with the die land area, where intermetallic particles and build up aluminum are present [11,12]. Pick-ups scratches often starts with a deposit and ends with a narrowing tail. As well explained by Peris [13], three types of pick-ups were identified, which are named as normal pick-up, die line pick-up, and lump pick-up. While normal pick-up occurs because of a localized sticking and tearing at the interface of the adhering aluminum layer and moving aluminum, die line pick-ups occurs from a deposit from the die then dragged along the extrudate surface leaving a scar and these pick-ups had die lines at both the head and the tail. Die line pick-ups were generally detected at the higher extrusion speeds, which are responsible of this defect. The lump pick-ups instead occur very rarely and consist of two parts, which are the lump and the tail. Alloy composition, tooling, equipment and the extrusion process parameters (such as pre-heat temperatures, extrusion speed, exit temperature, and die bearing conditions) have been listed as influencing factors affecting die pick-ups. Extrusion temperature is affecting the quantity and size of pick-ups, since increasing the temperature there is a softening of the Al matrix that leads to an easier loss of the intermetallic particles during extrusion. The particles may stick to the die surface and scratch the surface of the extrudate as well documented in previous literature works [11,13,14].

In the high solute alloys, due to the low melting point eutectic, tearing represents the biggest limitation to extrudability, while in low solute alloys the melting point is unlikely reached, therefore the occurrence of die lines and pick-ups are the limiting conditions for the extrusion velocity. Moreover, the high strength Al alloys are generally machined to remove the recrystallized layers therefore die lines have a secondary importance [11]. On the contrary, in the low solute Al alloys die lines and pick-ups represent the real limitation to the increase of the extrusion velocity, since the surface of these extrudates is not removed by machining and they often undergo anodizing treatment after extrusion, which needs a high surface quality [4,15–17].

In the hot extrusion process, the extrudability depends also on the alloy chemical composition. For the alloy 6060, which is one of the most used in the market of extruded profiles, previous studies [5,6,16] indicated that decreasing the Mg content, reduces the flow stress necessary to extrude the billet, thus leading to use lower extrusion temperatures. This, in turn, allows to increase the extrusion speed without reaching the critical temperature for the defects nucleation, improving in this way the alloy extrudability.

The minimum preheating temperature of the billet depends on the maximum available power of the press. In fact, the lower is the billet preheating temperature, the higher will be the flow stress of the material and, therefore, the extrusion pressure. Consequently, the minimum billet temperature is the one at which the power press is sufficient to induce the material flow. From an industrial perspective, it is suggested to start the extrusion process at a billet preheating temperature as lower as possible, but still allowing the breakout pressure to be less than 95% of the maximum power of the press [4].

In order to optimize the chemical composition of the 6060 alloy with the purpose to increase its extrudability, particular attention is paid to Mg and Si, i.e. the two principal alloying elements. As a matter of fact, the lower is the Mg and Si content, the higher will be the extrudability. As the experiments carried out by Reiso [6] account for, the maximum extrusion speed is reduced by 0.4 m/min per 0.01 wt% increase in the Si content of the alloy. An equivalent effect is observed for variations in the Mg content up to approximately 0.55 wt% as well. Above this concentration, further increase in the Mg content is even more detrimental to extrudability. The Mg and Si content affects both the solidus temperature and the flow stress of the alloy: the solidus temperature decreases, and the flow stress increases with increasing Mg and Si content. In particular, the solidus temperature is more sensitive to the Si content [18], while the flow stress is more sensitive to the Mg concentration [19]. On the other hand, it is also known that the best mechanical properties are obtained through a precipitation hardening treatment with a proper Mg and Si content, since the most hardening precipitates have a Mg:Si atomic ratio close to 1:1, playing these two elements a crucial role in satisfying the mechanical properties requirements [20–22].

The aim of the present investigation is to propose a new 6060 alloy composition, with a low Mg and Si content, resulting in an improvement of the alloy extrudability and fulfilling the requirements about the mechanical properties, thanks to the application of a proper ageing cycle.

2. Experimental procedure

Two different formulations of AA6060 alloy were direct-chill cast as 178 mm diameter logs at Fonderie Pandolfo in Maniago (Italy) using casting and homogenization parameters typical of industry standards for this type of alloy.

Table 1 – Chemical composition (wt%) of reference Alloy A and new formulated Alloy B.

	Mg	Si	Fe	Mn	Cu	Zn	Cr	Ti	Pb	Ni
Alloy A - Ref	0.42	0.46	0.25	0.033	0.022	0.037	0.009	0.018	0.003	0.006
Alloy B	0.35	0.43	0.21	0.035	0.020	0.030	0.007	0.019	0.009	0.007

Two alloy compositions were investigated in the present research, as shown in Table 1. Alloy A, is the reference alloy, whereas Alloy B is a new developed alloy. Its composition was chosen keeping the Mg and Si contents as close as possible to the minimum values allowed by the EN 573-3 standard (i.e. 0.35 wt% of Mg and 0.43 wt% of Si) [23]. As far as the other elements are concerned, the Mn content was chosen in a certain amount to promote the transformation of the undesirable intermetallic β-AlFeSi phases (present in the as-cast condition and detrimental to the extrudability) to α-AlFeSi particles (non-detrimental to the alloy extrudability) during the homogenization process [24–26]. A complete transformation of β-AlFeSi to α-AlFeSi was observed adding 0.08 wt % of Mn [27] but a lower amount is normally used since it leads to an increase in the flow stress and in quench sensitivity. Regarding the other alloying elements, typical Fe levels were used, whereas the amount of minor alloying elements such as Cu, Cr and Zn were kept as constant as possible, to simplify the comparison among the two alloys.

According to EN 755–2:2016 standard [28], for an extruded 6060 alloy profile, the minimum mechanical property requirements in T6 condition are: 190 MPa for UTS; 150 MPa for $\sigma_{y0.2}$; 8% for the elongation at fracture. There is not any specific minimum value for hardness and only a typical value of 70 HB is indicated.

To meet the minimum required mechanical properties, each alloy was submitted to three different thermal cycles [20]: a Standard cycle at 190 °C, a Dual Rate Ageing (DRA) cycle at 200°C–30 °C/h and a Dual Step ageing at 190 °C. DRA and Dual Step cycles were applied since they were identified as very promising for the improvement of the mechanical properties with respect to the ones obtained through the standard one [20]. The profiles from which tensile test samples were cut, were extruded at 28 m/min and the billet temperature was set at 470 °C for extrusion. Hardness and tensile properties were measured according to the standard tests methods BS EN ISO 6506 and ASTM B557M-15.

Surface defects evaluation was carried out by means of both visual observation and scanning electron microscope (SEM) on the region of the profile indicated by the red arrow in Fig. 2. The extrusion trials were performed at different speeds (from 26 m/min to 44 m/min) in an industrial extrusion 17.5 MN SMS Meer press, equipped with a 184 mm container. The extrusion parameters of the two alloys under study are reported in Tables 2 and 3. Extrusion speed tests were performed to assess the better extrudability achievable by the less alloyed composition (Alloy B) respect to the reference alloy (Alloy A). The evaluation of the surface defects (pick-ups, die-lines) on the extruded profiles has been carried out under a scanning electron microscope (SEM).

3. Results and discussion

3.1. *Mechanical properties*

As stated before, the Mg content affects the alloy extrudability, which increases as the Mg content is reduced. At the same time, lowering the Mg content to the minimum reduces the alloy strength. Therefore, a thermal treatment was considered necessary to increase this property. The hardness range of 6060 alloy in the as cast condition is 27–47 HB [29,30]. After solution treatment in the present research 35HB was measured while the hardness suggested by the Standard EN 755–2:2016 is 70 HB. This value can be achieved only through an optimized solution and ageing treatment. On the basis of a previous study [20] three different ageing cycles were selected, two novel and a standard one:

- Standard cycle at t = 145–355 min
- Dual Step 190 °C cycle at t = 325–355 min
- DRA 200°C–30 °C/h at t = 175–265 min

The ageing times were also chosen on the basis of a previous study to maximize the alloy strength [20].

The mechanical properties (UTS, $\sigma_{y0,2}$ and elongation%) measured though tensile testing are reported in Figs. 3–5 for the two alloys, as a function of the ageing cycles and ageing times used. Fig. 3 refers to the properties obtained applying the standard ageing cycle, while in Fig. 4 the mechanical properties obtained after the DRA cycle, and in Fig. 5 after the Dual Rate ageing cycle were presented. All the mechanical properties of these alloys comply with the minimum

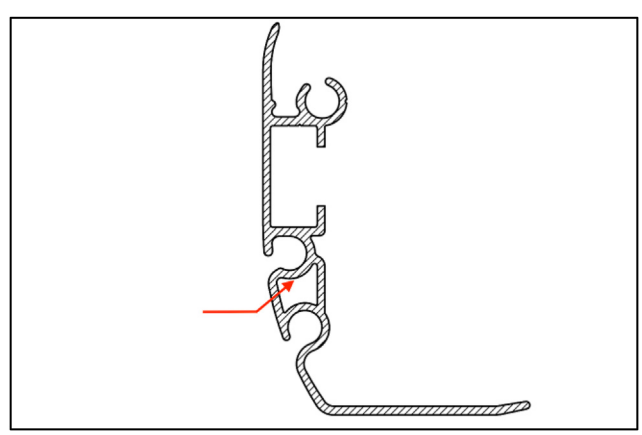

Fig. 2 – Profile shape with the red arrow indicating the region where the surface defects were examined.

Table 2 – Extrusion parameters recorded during the speed test of Alloy A.

Alloy A					
Set billet temperature (°C)	Recorded front billet temperature (°C)	Recorded rear billet temperature (°C)	Set pulled speed (m/min)	Billet length (mm)	Recorded extrusion time (s)
440	441	427	26	687	115
440	437	427	30	682	98
440	438	430	33	686	92
440	440	424	36	686	87
440	436	423	39	684	82
440	439	434	40	685	80
440	438	427	42	682	76
440	440	435	44	683	73

requirements for a 6060 Al alloy, which are indicated with a dotted line in each graph; only Alloy B after ageing with the standard cycle needs a minimum ageing time of 175 min to reach the requested UTS. For this alloy, the increase in mechanical properties provided by the DRA 200°C–30 °C/h cycle compared to the standard cycle is significant. This difference can be attributed to the effect of natural ageing: the lower is the solute content (Mg + Si) of the alloy, the greater will be the influence of the prolonged room temperature storage in enhancing the mechanical properties of the alloy [31–33]. As expected, Alloy A has better mechanical properties (UTS and $\sigma_{y0,2}$) for all the ageing conditions, since it has a higher Mg + Si content. Concerning elongation, the two alloys show similar values in all the ageing conditions with no appreciable differences related to their chemical composition. These values are largely higher than the minimum required by the standard EN 755–2:2016 (8%) [28].

Standard deviations of tensile data are extremely small: for UTS, standard deviations are between ±0.7 MPa and ±1.7 MPa (maximum standard deviation measured), for $\sigma_{y0,2}$ they go from ±1 MPa and ±2.5 MPa and for elongation they are between ± 0.25% and ±0.7%.

The higher mechanical properties of the reference alloy are due to the chemical composition of this alloy since a higher amount of Mg + Si results in a more abundant precipitation of intermetallics as extensively reported in a previous paper [20]. A comparison between the Mg_5Si_6 hardening precipitates observed under the TEM in Alloy A and Alloy B, after aging through Dual Step cycle for 355 min, is reported in Fig. 6a and b.

3.2. *Die line pick-ups*

To assess the extrudability of the alloys under study, extrusion tests for the evaluation of the surface defects were carried out, checking the appearance of surface defects (pick-ups, die-lines) on the extruded profiles. The defects observed are die lines and die line pick-ups as shown in the SEM pictures of Figs. 7–9.

Increasing the extrusion velocity, it was observed a transition from a defect-free surface to firstly micro die lines and then macro die lines with pick-ups phenomena (die line pick-ups). No tearing (hot shortness) was detected on the surface of the profiles also on those extruded at the maximum velocity. In order to establish the influence of the extrusion speed, which is related to the effective extrusion temperature, on the occurrence of surface defects as die lines, the following simplified approach is proposed.

First, the average strain rate in the extrudate is evaluated by the following relationship [34]:

$$\dot{\varepsilon} = \frac{6 \cdot v_0 \cdot D_0^2 \cdot tg\alpha}{D_0^3 - D_f^3} \cdot lnR^* \quad (1)$$

where:

v_0 is the extrusion speed (refer Tables 2 and 3).

D_0 is the initial billet diameter (178 mm).

D_f is the diameter of the "equivalent billet", i.e. the billet having the same area of the extruded profile

α is the die half-opening angle (simply given by: 54 + 3.45 lnR*, [35]).

R* is the extrusion ratio.

Table 3 – Extrusion parameters recorded during the speed test of Alloy B.

Alloy B					
Set billet temperature (°C)	Recorded front billet temperature (°C)	Recorded rear billet temperature (°C)	Set pulled speed (m/min)	Billet length (mm)	Recorded extrusion time (s)
430	428	412	26	695	114
430	430	419	30	693	99
430	426	416	33	694	93
430	430	418	36	692	88
430	426	415	39	691	82
430	427	421	40	688	81
430	429	418	42	688	77
430	428	421	44	688	73

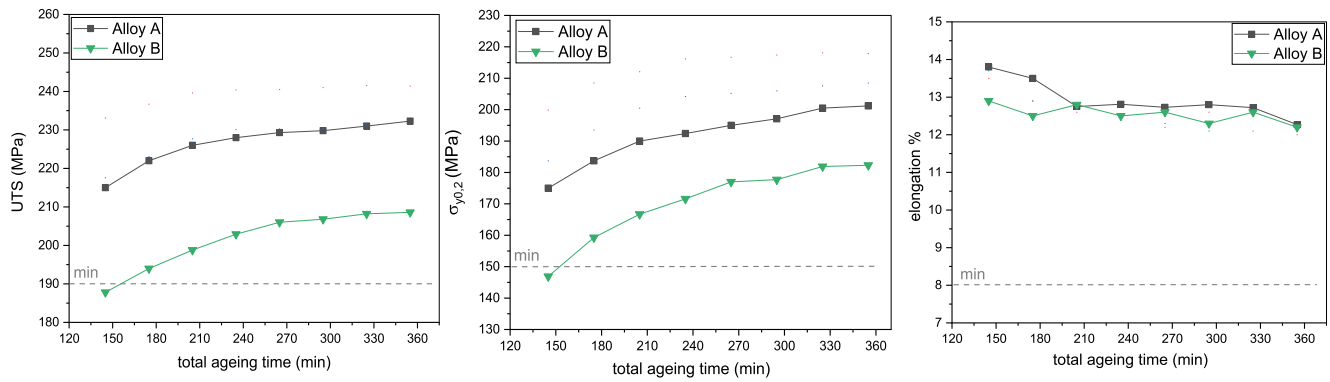

Fig. 3 – UTS (a), Rp0,2 (b) and elongation % (c) of the four alloys aged through the standard cycle at different times.

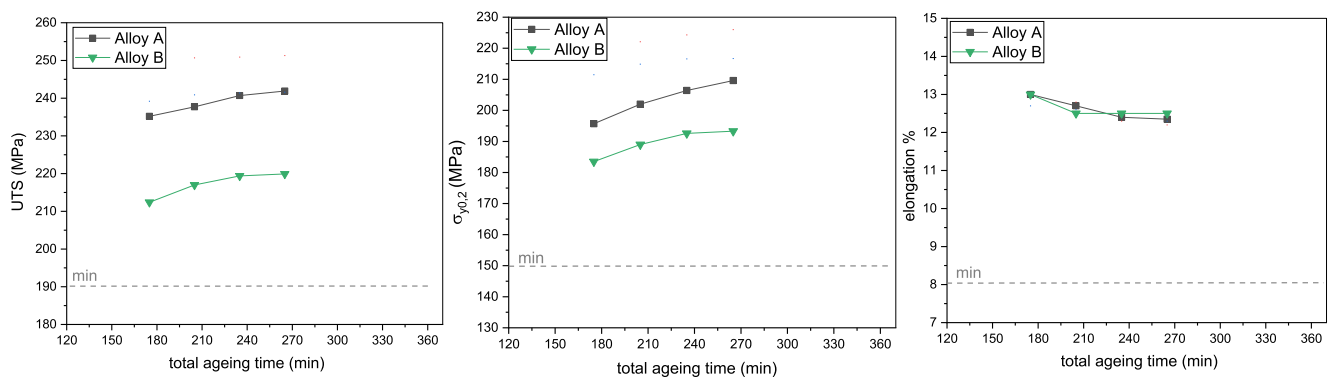

Fig. 4 – UTS (a), Rp0,2 (b) and elongation % (c) of the four alloys aged through the DRA 200 °C–30 °C/h cycle at different times.

The $\dot{\varepsilon}$ values obtained from the relationship (1) were used to calculate the corresponding Zener-Hollomon parameter Z:

$$Z = \dot{\varepsilon}\exp\left(\frac{\Delta H}{RT}\right) \tag{2}$$

where:

ΔH is the activation energy for hot deformation of the alloy (derived from Ref. [36] for Alloy A).

R is the gas constant.

T is the absolute temperature.

The Z parameter has been used in the constitutive equation to find the mean flow stress $\bar{\sigma}$ according to the formula proposed by Sellars and Tegart [37] and then modified by Sheppard and Wright [38]:

$$Z = \bar{\varepsilon}\exp\left(\frac{\Delta H}{RT}\right) = A[\sinh(\alpha\sigma)]^n \tag{3}$$

with the values of the constant A, n and ΔH taken from Ref. 36.

In case of Alloy B, no specific literature data are available to estimate Z and the mean flow stress with Eqs. (2) and (3). Therefore, the mean flow stress for Alloy B was obtained from the values calculated for Alloy A, dividing them by a factor k, defined by the ratio between hardness HB of Alloy A and that of Alloy B: k = 30/34 = 0.88. This approach simply considers

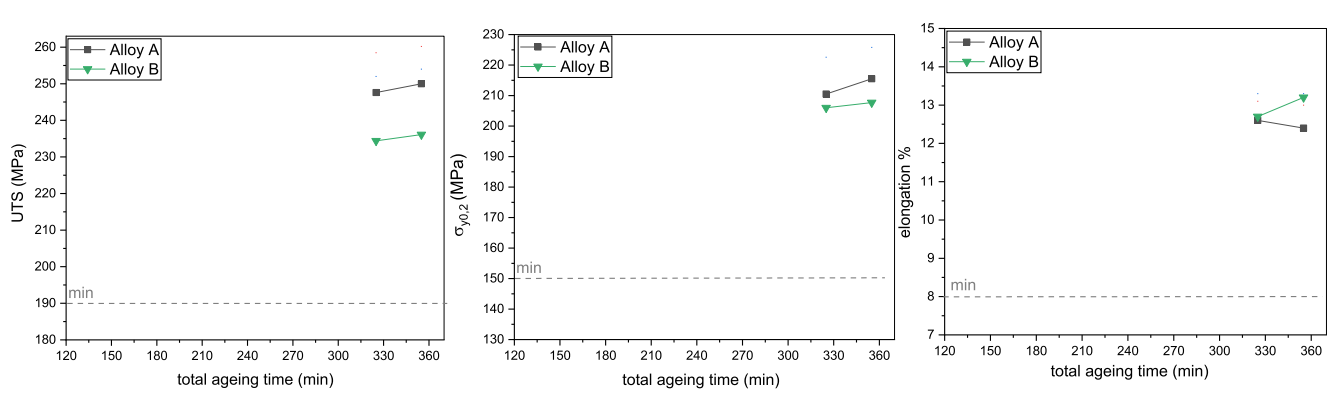

Fig. 5 – UTS (a), Rp0,2 (b) and elongation % (c) of the four alloys aged through the Dual Step 190 °C cycle at two different times.

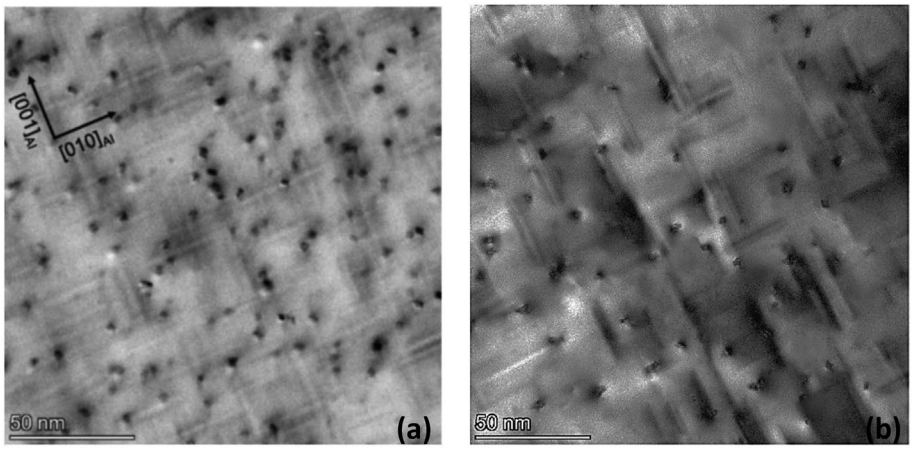

Fig. 6 – TEM micrographs of Alloy A (a) and Alloy B (b) aged through Dual Step cycle for 355 min.

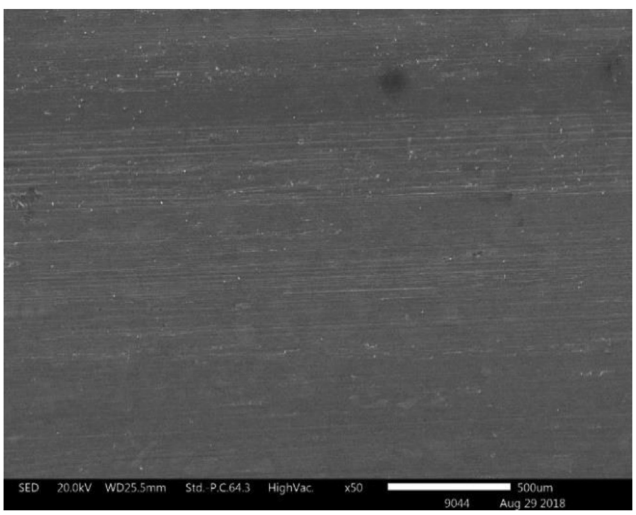

Fig. 7 – Acceptable micro die lines (Alloy B extruded at 36 m/min).

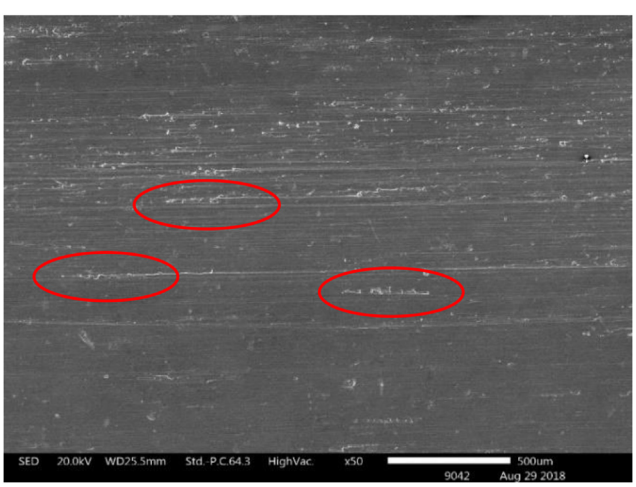

Fig. 8 – Not acceptable micro die lines (Alloy B extruded at 39 m/min).

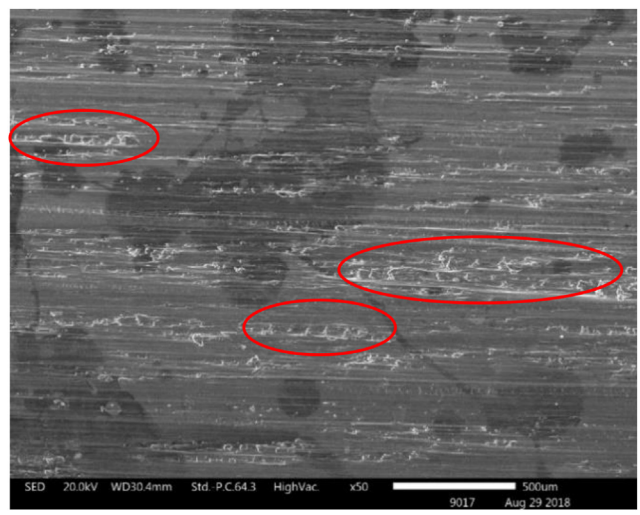

Fig. 9 – Macro die lines with some die line pick-ups (surrounded) (Alloy A extruded at 44 m/min).

that the flow stress of the alloys under study is proportional to their hardness, even at high temperature.

From the $\bar{\sigma}$ values, the nominal extrusion pressure p_0 was calculated according to [35]:

Table 4 – Exit temperatures T* as a function of the extrusion speed for Alloy A.

Extrusion speed [m/min]	T^*_{front} (°C) after 4 iterations	T^*_{rear} (°C) after 4 iterations	T^*_{mean} (°C)
26	557	555	556
30	564	556	560
33	566	559	563
36	568	555	562
39	565	558	561
40	568	564	566
42	567	558	565
44	569	565	567

Table 5 – exit temperatures T* as a function of the extrusion speed for Alloy B.

Extrusion speed [m/min]	T^*_{front} (°C) after 4 iterations	T^*_{rear} (°C) after 4 iterations	T^*_{mean} (°C)
26	535	530	533
30	540	537	539
33	543	535	539
36	541	537	539
39	544	540	542
40	545	540	542
42	547	538	542
44	546	540	543

$$p0 = \bar{\sigma} \cdot (a + b \ln R^*) \quad (4)$$

where a and b are respectively 1.06 and 1.55 for unlubricated conditions [35] and R* is the extrusion ratio. The p_0 values were then used to calculate the extrusion pressure, p_{ext}, which takes into account the friction at the metal-container interface (5):

$$pext = p0 + pext = p0 + p0\frac{4\mu L}{D_0} = p0\left(1 + \frac{4\mu L}{D_0}\right) \quad (5)$$

where:

μ is the friction coefficient at the billet–container interface (it is set to 0.08 according to data provided by Sellars and Sheppard in case of hot extrusion of Al alloys without lubricant [39]).

L is remaining length of the billet in the container, which has its maximum when the extrusion process starts and therefore L is the initial length of the billet.

D_0 is the internal diameter of the container.

The p_0 values are also used to calculate the ΔT_{def} through formula (6) [40] which indicates the temperature rise due to the deformation process, considering it adiabatic:

$$\Delta T_{def} = 0.9\frac{p_0}{\rho c} \quad (6)$$

where:

ρ is the alloy density (2.7 g/cm^3).

c is the alloy specific heat capacity (898 J/kg*K).

Neglecting thermal losses, the actual process temperature T* is the sum of the preheating temperature T_0 and two contributions, the first given by the plastic deformation (1/2 ΔT_{def} assuming a linear increase of the temperature in the die) and the second given by friction (ΔT_μ), which is expressed by [40]:

$$\Delta T\mu = \frac{1}{2}\frac{p_{ext} - p_0}{\rho c} \quad (7)$$

Therefore, the extruded profile exit temperature can be calculated as:

$$T^* = T0 + ½\Delta Tdef + \Delta T\mu \quad (8)$$

The calculation of T* has been carried out for the different extrusion velocities reported in Tables 2 and 3 (i.e. from 26 m/min to 44 m/min) for the front billet temperature ($T_{0\ front}$) and the rear billet temperature ($T_{0\ rear}$) with an iterative process since the T*values, calculated in the first iteration inserting as T_0 the temperatures reported in the second and third columns of Tables 2 and 3, were used for the recalculation of Z (second iteration) and, in turn, new values of $\bar{\sigma}$, p_0, p_{ext}, and T*. The iterations were stopped when the difference in the calculated values was lower than 5%. The final T* values (front, rear and mean value) are summarized in Tables 4 and 5 for Alloy A and Alloy B, respectively.

To establish a criterion for the occurrence of the plastic deformation phenomena (die lines, pick-ups) observed on the surface of the extrudates, the mean value between T^*_{front} and T^*_{rear} has been considered, since it's not possible to determine whether the surface defects occur on the front or the back part of the billet during the extrusion process.

The mean values of the exit temperature were correlated with the observation of surface defects on the extruded profiles, as shown in Table 6 and in the graph of Fig. 10, in which the two alloys are compared.

- Very little, scarcely visible die lines, which, from the industrial quality point of view, are fully acceptable and do not result in a profile discard, as in the case of Alloy B for extrusion speeds from 30 to 36 m/min (an example is shown in Fig. 7);
- Micro die lines with some very small pick-ups, which are not accepted and result in a product rejection (an example is reported in Fig. 8 on which some pick-ups are indicated);
- Macro die lines, characterized by a more intense surface deformation with more evident pick-ups as those indicated

Table 6 – Exit temperature T* of Alloy A and Alloy B correlated with the defects observed on the surface of the extruded profiles.

Extrusion speed [m/min]	Alloy A		Alloy B	
	T^*_{mean} (°C)	surface defects evaluation	T^*_{mean} (°C)	surface defects evaluation
26	557	micro die lines	533	no die lines
30	564	micro die lines	539	acceptable die lines
33	566	macro d.l. + pick-up	539	acceptable die lines
36	568	macro d.l. + pick-up	539	acceptable die lines
39	565	macro d.l. + pick-up	542	micro die lines
40	568	macro d.l. + pick-up	542	micro die lines
42	567	macro d.l. + pick-up	542	micro die lines
44	569	macro d.l. + pick-up	543	micro die lines

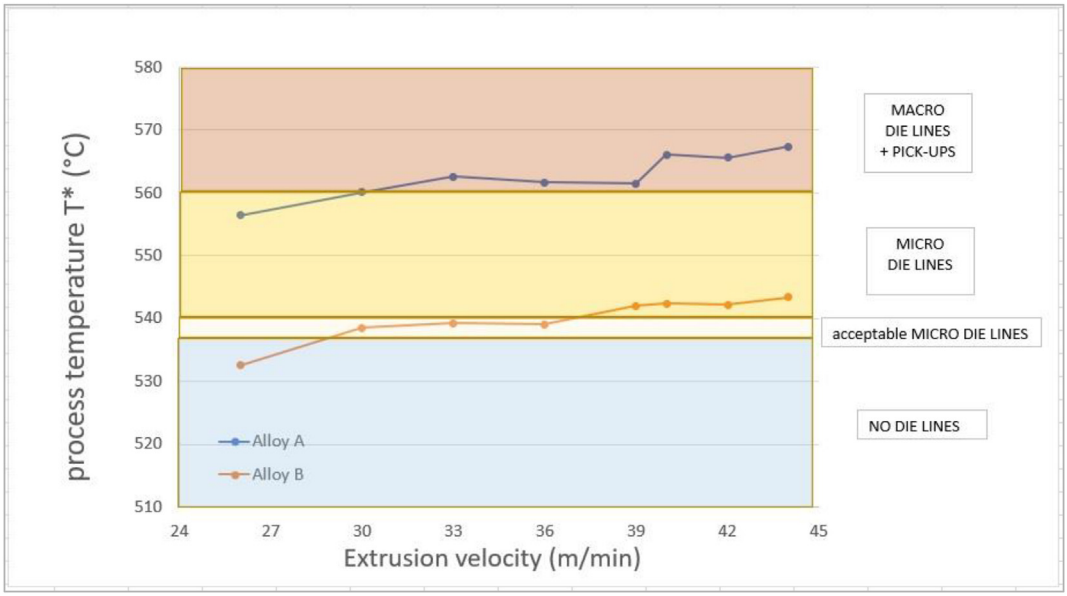

Fig. 10 – Process extrusion temperature T* vs. extrusion velocity.The phenomena observed on the surface of the extrudates are the following (listed here from the less to the most damaging).

in Fig. 9 (die line pick-ups). Evidently, also in this case, the extruded profile is considered not fulfilling the quality requirements and it's discarded.

The comparison between the two alloys shows that Alloy B can be extruded up to 36 m/min without the occurrence of any defect causing a product rejection, while Alloy A already shows micro die lines at 26 m/min. This leads to a significant increase of the industrial productivity if Alloy B is used instead of the reference Alloy A.

A comparison which highlights the evident difference between the two alloys is reported in Table 7 where the surfaces

Table 7 – Comparison between Alloy A and Alloy B extruded at the same velocities of 30 m/min and 36 m/min.

Extrusion velocity	Alloy A	Alloy B
30 m/min	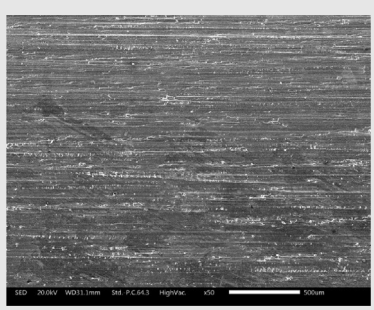	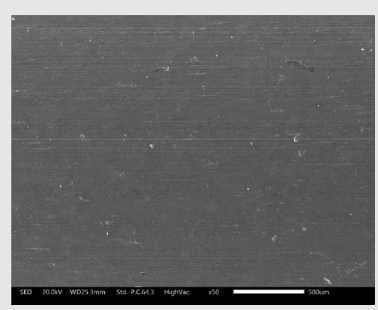
36 m/min	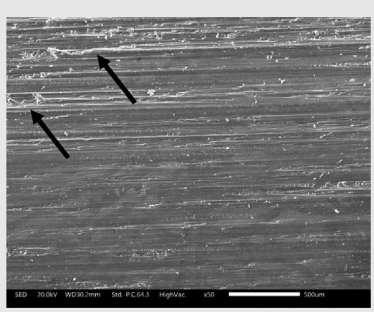	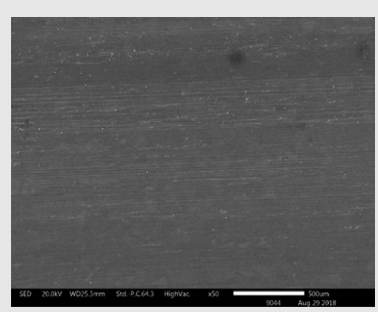

of Alloy A and Alloy B are shown after extrusion at the same two velocities of 30 and 36 m/min. As can be seen there are evident die-lines and pick-ups only on the surface of Alloy A. Pick-ups are less pronounced at the extrusion speed of 30 m/min than at 36 m/min. In this last specimen they reveal a deeper ploughing phenomenon, as indicate by the arrows.

From the graph of Fig. 10 a clear transition is observed for Alloy B from a "safe" extrusion temperature range up to 540 °C, where defects are not present or so minimal that can be accepted, to a higher temperature range (540–560 °C) characterized by the occurrence of micro die lines, and then to further higher temperatures (T > 560 °C), where a more severe surface plastic deformation is observed. All the process temperatures T* obtained by the temperature criterion are far from the melting temperature of the two alloys, determined through a differential scanning calorimetry DSC analysis (Fig. 11), which is close to 630 °C. Thus, the present model excludes the possibility to have hot shortness phenomena and this is confirmed by the SEM analysis of the defects observed on the surface of the extrudates.

In the light of the data reported, it is possible to surmise that the new Alloy B provides a potential maximum extrusion speed to be significantly higher than the standard Alloy A. From an industrial perspective, such a gain in extrusion speed leads to a reduction in extrusion time and, therefore, to an increase in productivity.

The higher maximum extrusion speed of the Alloy B profile proves the influence of Mg and Si – i.e. the two main alloying elements – on this characteristic, being higher the extrudability when the alloy is poorer in these elements.

Moreover, combining the DRA 200°C–30 °C/h ageing cycle with Alloy B (Fig. 4) allows to meet the minimum mechanical requirements for a quite short ageing time of 175 min, leading to an ultimate tensile strength and a yield strength respectively 11.8% and 22.8% higher than the minimum requirements.

Vice versa, combining Alloy B with the standard ageing cycle, the minimum mechanical requirements are barely satisfied: for a total ageing time of 175 min, the ultimate tensile strength and the yield strength are respectively just 2.1% and 6.2% higher than the relative minimum requirements.

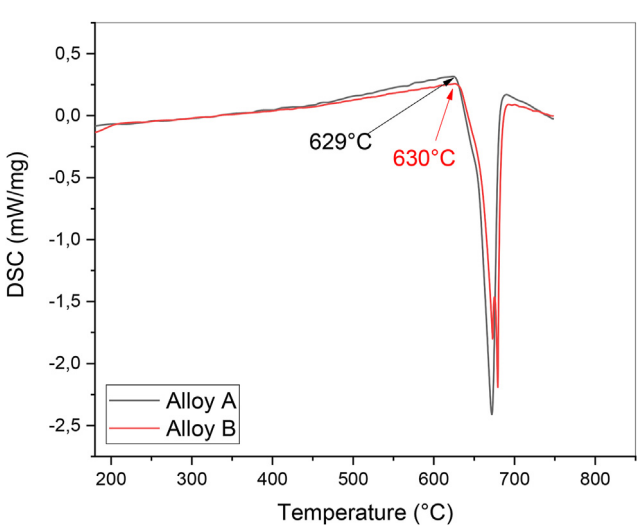

Fig. 11 – DSC curve of Alloy A and Alloy B.

Therefore, at an industrial scale, in order to have a certain margin requirement, the use of Alloy B is effective only in combination with the new DRA 200°C–30 °C/h ageing cycle. On the other side, should a standard cycle be used, Alloy B would require either an increase in the total ageing time or an increase in Si content to enhance the mechanical properties. Still, this would lead to a reduction in productivity.

4. Conclusions

The main results obtained from the comparison of two different AA6060 alloys, a reference alloy (Alloy A) and a new developed alloy (Alloy B), in which the amount of Mg and Si was set at the minimum required by the standard, are the following:

- Alloy A, which has a higher Mg + Si content shows better mechanical properties, after all the ageing conditions, but a worse extrudability than Alloy B, resulting in the appearance of surface defects even at the minimum extrusion velocity tested of 26 m/min.
- Alloy B, which has the lowest Mg + Si content, shows the highest extrudability with a significant increase in the maximum extrusion speed. Applying the DRA 200°C–30 °C/h ageing cycle to this alloy for a quite short ageing time of 175 min, allows to fulfil the minimum mechanical properties requirements, leading to an ultimate tensile strength and a yield strength respectively 11.8% and 22.8% higher than the minimum requested values.

Therefore, at an industrial scale, the use of Alloy B is profitable only in combination with the new DRA 200°C–30 °C/h ageing cycle, leading to the combination of higher industrial productivity and interesting mechanical properties for short ageing times.

Starting from experimental data recorded during the extrusion process, a temperature model was proposed to establish the occurrence of the defects on the surface of the extrudates.

Declaration of Competing Interest

The authors declare that they have no known competing financial interests or personal relationships that could have appeared to influence the work reported in this paper.

REFERENCES

[1] Saha P. Aluminum extrusion technology. ASM Int; 2000.
[2] Lefstad M. Metallurgical speed limitations during the extrusion of AlMgSi-alloys. 1993.
[3] Arif AF, Sheikh AK, Qamar SZ. Product defects in aluminum extrusion and its impact on product defects in aluminum extrusion and its impact on operational cost. 6th Saudi Eng Conf 2002;18.

[4] Fourmann J defects affecting extruded surface - speed cracking. Light Met Age 40–41.
[5] Tundal U, Reiso O, Hoff E, Dickson R, Devadas C, et al. High speed alloys: on the optimization of 6xxx alloys for medium strength requirements, hydro aluminium technology centre. Proc 10th Int Alum Extrus Technol Semin May 15-18, Miami Beach, Florida Washington DC Alum Assoc 2012;12:21–33.
[6] Reiso O. The effect of composition and homogenization treatment on extrudability of AlMgSi alloys. Proc 3rd Int Alum Extrus Technol Semin April 24-26. Atlanta: Georg Alum Assoc; 1984. p. 31–40.
[7] Reiso O. The effect of billet preheating practice on extrudability of AlMgSi alloys. Proc 4th Int Alum Extrus Technol Semin April 11-14. Chicago: Illinois Alum Assoc; 1988. p. 287–95.
[8] Misiolek WZ, University L, Kelly RM, Co W. Extrusion of aluminum alloys. 2005. https://doi.org/10.1361/asmhba0004015.
[9] Akeret Pms R. Unconventional extrusion processes for the harder aluminum alloys. Light Met Pt I-II Age 1973:15–8.
[10] Tempelman E, Shercliff H, van Eyben BN. Extrusion of metals. Manuf Des 2014:69–83. https://doi.org/10.1016/B978-0-08-099922-7.00005-6.
[11] Clode MP, Sheppard T. Formation of die lines during extrusion of AA6063. Mater Sci Technol 1990;6:755–63. https://doi.org/10.1179/mst.1990.6.8.755.
[12] Sheppard T, Clode MP. The origin of surface defects during extrusion of AA6063 alloy. Proc 4th Int Alum Extrus Technol Semin Alum Ass Alum Extruders Counc 1988;2:329–41.
[13] Peris R, Chen ZW, Pasang T, Hand C, Chen S, Hayward B, et al. Effects of process conditions on die pick-up formed during extrusion of aluminum alloy AA6060. Aluminum Extr Council; 2007. p. 271–8.
[14] Degarmo EP, Black JT, Kohser RA. Materials and process in manufactoring. Mater Process Manuf 2003;383.
[15] Fourmann J, Tinto R Defects affecting extruded surface - pick-up. Light Met Age 28–29.
[16] Parson NC, Hankin JD. Bryant J the metallurgical background to Problems occurring during the extrusion of 6XXX alloys. Chicago, Illinois, USA: Proc 5th Alum Extrus Technol Semin; 1992. p. 13–23. May 19-22, 1992.
[17] Parson NC, Jowett CW, Fraser WC, Pelow CV. Surface defects on 6XXX alloy extrusions. Proc 6th Alum Extrus Technol Semin 1996;1996:57–67. Chicago, Illinois USA May 14-17.
[18] Phillips HWL. Annotated equilibrium diagrams of some aluminium alloy systems. London: Institute of Metals; 1959.
[19] Castle AF, Lang G. The influence of various alloying elements and heat treatments on the hot-workability of binary aluminum alloys during extrusion. Aluminium 1977;53:535–9.
[20] Menapace C, Bernard F, Lusa M, Ischia G, Straffelini G. Effect of a dual-rate ageing treatment on the tensile properties of a commercial 6060 Al alloy. Mater Sci Eng A 2021;819:141468. https://doi.org/10.1016/J.MSEA.2021.141468.
[21] Marioara CD, Andersen SJ, Zandbergen HW, Holmestad R. The influence of alloy composition on precipitates of the Al-Mg-Si system. Metall Mater Trans 2005;363:691–702. https://doi.org/10.1007/S11661-005-0185-1.
[22] Andersen SJ, Zandbergen HW, Jansen J, Traholt C, Tundal U, Reiso O, et al. The crystal structure of the β″ phase in Al-Mg-Si Alloys. Acta Mater 1998;46:3283–98. https://doi.org/10.1016/S1359-6454(97)00493-X.
[23] Uni En 573-3. Aluminium and aluminium alloys. Chemical composition and form of wrought products. Committe Europeen de Normalisation; 2009.
[24] Zajac S, Hutchinson B, Johansson A, Gullman L-O. Microstructure control and extrudability of Al–Mg–Si alloys microalloyed with manganese. Mater Sci Technol 1994;10:323–33. https://doi.org/10.1179/MST.1994.10.4.323.
[25] Aydi L, Khlif M, Bradai C, Spigarelli S, Cabibbo M, El Mehtedi M, et al. Mechanical properties and microstructure of primary and secondary AA6063 aluminum alloy after extrusion and T5 heat treatment. Mater Today Proc 2015;2:4890–7. https://doi.org/10.1016/J.MATPR.2015.10.044.
[26] Liu CL, Azizi-Alizamini H, Parson NC, Poole WJ. The effect of Mn on microstructure evolution during homogenization of Al-Mg-Si-Mn alloys. Mater Sci Forum 2014;794–796:1199–204. https://doi.org/10.4028/WWW.SCIENTIFIC.NET/MSF.794-796.1199.
[27] Devadas C, Musulin I, Celliers O. Prediction of the microstructure of DC cast 6063 billets and its effect on extrusion processes. Orlando: Proc 5th Int Alum Extrus Technol Semin May 18-21; 1992. p. 121–8. Florida.
[28] Uni En 755-2. Aluminium and aluminium alloys. In: Extruded rod/bar, tube and profiles Mechanical properties. Committe Europeen de Normalisation; 2016.
[29] Mondolfo LF. Aluminum alloys. 1976. https://doi.org/10.1016/C2013-0-04239-9.
[30] Silva MS, Barbosa C, Acselrad O, Pereira LC. Effect of chemical composition variation on microstructure and mechanical properties of a 6060 aluminum alloy. J Mater Eng Perform 2004;13:129–34. https://doi.org/10.1361/10599490418307.
[31] Røyset J, Stene T, Sæter JA, Reiso O. The effect of intermediate storage temperature and time on the age hardening response of Al-Mg-Si alloys. Mater Sci Forum 2006;519–521:239–44. https://doi.org/10.4028/WWW.SCIENTIFIC.NET/MSF.519-521.239.
[32] Hatta H, Matsuda S, Yoshida H. Two-step aging behaviors of Al-Mg-Si alloy extrusions. Keikinzoku/J Japan Inst Light Met 2006;56:667–72. https://doi.org/10.2464/JILM.56.667.
[33] Lai YX, Jiang BC, Liu CH, Chen ZK, Wu CL, Chen JH, et al. Low-alloy-correlated reversal of the precipitation sequence in Al-Mg-Si alloys. J Alloys Compd 2017;701:94–8. https://doi.org/10.1016/J.JALLCOM.2017.01.095.
[34] Dieter GE, Bacon D. Mechanical metallurgy si metric. Edition. McGraw-Hili Book Company; 1988. p. 767.
[35] Kalpakjian S, Schmid S. Manufacturing engineering and technology. 6th edition. Addision-Wesley Publishing Company Inc; 1995.
[36] Sheppard T, Jackson A. Constitutive equations for use in prediction of flow stress during extrusion of aluminium alloys. Mater Sci Technol 1997;13:203–9. https://doi.org/10.1179/mst.1997.13.3.203.
[37] Sellars CM, Tegart WJM. Hot workability. Int Metall Rev 1972;17:1–24. https://doi.org/10.1179/IMTLR.1972.17.1.1.
[38] Sheppard T, Wright DS. Determination of flow stress: Part 1 constitutive equation for aluminium alloys at elevated temperatures. Technol 1979;6:215–23. https://doi.org/10.1179/030716979803276264.
[39] Sheppard T. Temperature and speed effects in hot extrusion of aluminium alloys. Technol 1981;8:130–41. https://doi.org/10.1179/030716981803276009.
[40] Sheppard T. Temperature changes occurring during extrusion of metals: comparison of bulk, numerical, and integral profile predictions with experimental data. Mater Sci Technol 1999;15:459–63. https://doi.org/10.1179/026708399101505941.